Origin of variation in switching voltages in threshold-switching phenomena of VO2 thin films

S. B. Lee, K. Kim, J. S. Oh, B. Kahng, and J. S. Lee

Related Articles

Comprehensive study of the metal-insulator transition in pulsed laser deposited epitaxial VO2 thin films
J. Appl. Phys. 113, 043707 (2013)

Tunable electronic properties of ZnO nanowires and nanotubes under a transverse electric field
J. Appl. Phys. 113, 034301 (2013)

An absence of the Anderson transition in high-resistance alloys with a high electron density
Low Temp. Phys. 39, 2 (2013)

Tuning metal-insulator transition by one dimensional alignment of giant electronic domains in artificially size-controlled epitaxial VO2 wires
Appl. Phys. Lett. 101, 263111 (2012)

Studies on temperature dependent semiconductor to metal transitions in ZnO thin films sparsely doped with Al
J. Appl. Phys. 112, 103706 (2012)

Additional information on Appl. Phys. Lett.

Journal Homepage: http://apl.aip.org/

Journal Information: http://apl.aip.org/about/about_the_journal

Top downloads: http://apl.aip.org/features/most_downloaded

Information for Authors: http://apl.aip.org/authors
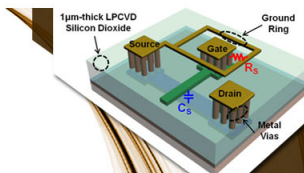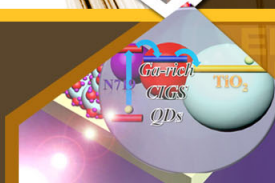
Origin of variation in switching voltages in threshold-switching phenomena of VO$_2$ thin films

S. B. Lee,[1,2,a)] K. Kim,[2] J. S. Oh,[1,2] B. Kahng,[2] and J. S. Lee[3,b)]

[1]*IBS-CFICES, Seoul National University, Seoul 151-747, South Korea*
[2]*Department of Physics and Astronomy, Seoul National University, Seoul 151-747, South Korea*
[3]*School of Physics, Korea Institute for Advanced Study, Seoul 130-722, South Korea*

We investigated the origin of the variation in switching voltages in threshold-switching of VO$_2$ thin films. When a triangular-waveform voltage signal was applied, the current changed abruptly at two switching voltages, i.e., V_{ON} (insulator-to-metal) and V_{OFF} (metal-to-insulator). V_{ON} and V_{OFF} were measured by changing the period of the voltage signal, the temperature of the environment, and the load resistance. We observed that either V_{ON} or V_{OFF} varied significantly and had different dependences with respect to the external parameters. Based on the mechanism of the metal–insulator transition induced by Joule heating, numerical simulations were performed, which quantitatively reproduced all of the experimental results. From the simulation analysis, the variation in the switching voltages for threshold-switching was determined to be thermal in origin. © 2013 American Institute of Physics. [http://dx.doi.org/10.1063/1.4790842]

Threshold-switching is a volatile and reversible transition that occurs between the high- and low-resistance states.[1,2] The phenomenon is of great interest in condensed matter research because it causes significant changes in a material's electrical, optical, and mechanical properties and can be triggered by different external (thermal, electrical, or optical) stimuli. VO$_2$ is an example of a typical threshold-switching material.[1,2] VO$_2$ threshold-switching has been widely studied for various technological applications, such as electrical switches,[3,4] smart windows,[5] terahertz nanoantennas,[6] and memory metamaterials.[7]

To utilize the VO$_2$ threshold-switching for practical purposes, it is important to understand and control detailed properties of the phenomenon. In particular, control over the switching voltages, where abrupt current changes occur by application of electric fields, is crucially important for stable performance of VO$_2$ devices.[3,4] Despite such importance, intentional control over the switching voltages has not been quantitatively investigated to date. We address a key question in this work: can the switching voltages be varied by changing the external parameters, and if they can, what is the origin of the variation?

Here, we measured the switching voltages of threshold-switching in VO$_2$ thin films by applying a triangular-waveform voltage signal. We found significant variation in switching voltages with changes in the period of the voltage signal, environmental temperature, and load resistance. We reproduced all of these experimental findings using numerical simulations based on the mechanism of the metal–insulator transition induced by Joule heating. Our simulation results indicated that the variation in the switching voltages was determined by the generation and dissipation of Joule heating.

We deposited insulating VO$_2$ thin films onto Al$_2$O$_3$ (0001) substrates by pulsed laser deposition. The films were grown at a substrate temperature of 560 °C, an oxygen pressure of 6.5 mTorr, and a laser fluence of 1.5 J/cm^2. Photolithography and DC-magnetron sputtering were used to deposit 200 × 200-μm^2-area Pt electrodes onto the VO$_2$ thin films. The inset of Fig. 1(a) shows a schematic diagram of the Pt/VO$_2$/Al$_2$O$_3$ sample geometry and the electrical
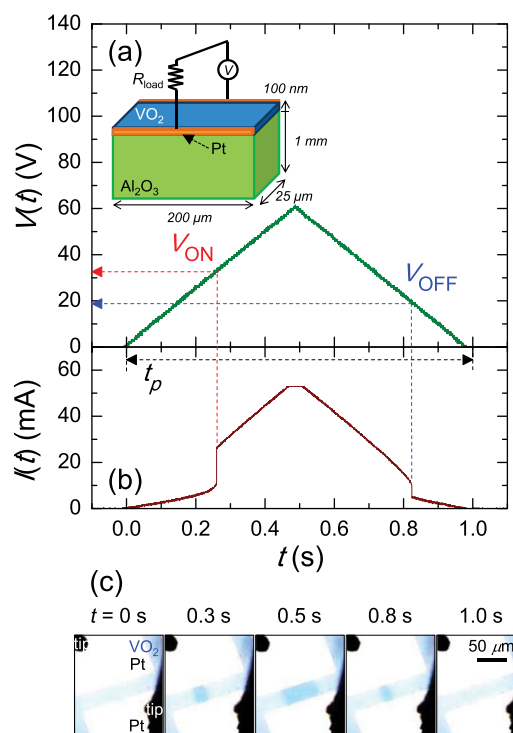

FIG. 1. (a) A triangular-waveform voltage signal $V(t)$ with a fixed amplitude of 60 V and period t_p. Inset shows a schematic of the Pt/VO$_2$/Al$_2$O$_3$ sample geometry and electrical measurement setup. (b) The resulting current $I(t)$, restricted by the current flow of the load resistor. We defined the switching voltages V_{ON} and V_{OFF} as $V(t)$ at the time when $I(t)$ abruptly increased and decreased, respectively. (c) Procedure for formation of a channel on the surface of the VO$_2$ thin film; the channel has different optical properties than its surroundings.

a)Electronic mail: sblee81@snu.ac.kr.
b)Electronic mail: jslee@kias.re.kr.

102, 063501-1

measurement setup. For all of the electrical measurements, we selected two adjacent Pt electrodes, which were separated by 25 μm.

Threshold-switching was induced in the VO$_2$ thin films by applying a triangular-waveform voltage signal, as shown in Figs. 1(a) and 1(b). The triangular-waveform voltage signal $V(t)$ was swept linearly over time t, with a fixed amplitude of $V_{max} = 60$ V, using a Yokogawa FG300 synthesized function generator (Fig. 1(a)). The resulting current $I(t)$ was measured simultaneously, using a Yokogawa DL7100 digital oscilloscope (Fig. 1(b)). To avoid pulse shape deformation, the impedance was matched using an nF HSA4101 high-speed bipolar amplifier. An abrupt increase and decrease in $I(t)$ occurred at $V(t) = V_{ON}$ and V_{OFF}, indicating insulator-to-metal and metal-to-insulator transitions, respectively. The current flow was limited by connecting a load resistor of resistance value R_{load} in series; this prevented permanent sample damage by an abrupt current jump at V_{ON}.

We observed the formation of a channel with different optical property between the two electrodes when the VO$_2$ thin film became metallic. Figure 1(c) shows one example of sequential snapshots of channel formation during the voltage application (Fig. 1(a)). Color changes were monitored in the VO$_2$ thin film by an optical charge-coupled device camera. The first snapshot shows that there was no channel on the VO$_2$ film surface at $V(0) = 0$ V. When the VO$_2$ thin film became macroscopically metallic at $V(t) > V_{ON}$, a darker localized channel appeared in the film, as shown in the second snapshot. Further increases in $V(t)$ made the channel wider (third snapshot); however, the channel width became narrower when $V(t)$ decreased (fourth snapshot). When the VO$_2$ thin film became macroscopically insulating at $V(t) < V_{OFF}$, the channel disappeared (fifth snapshot). This analysis indicated that the channel was highly conducting, compared with other regions; i.e., the threshold-switching of the VO$_2$ thin film was accompanied by conducting channel formation and rupture.

To collect information on the external parameters affecting the switching voltages, we first measured V_{ON} and V_{OFF} by changing t_p, the period of the triangular-waveform voltage signal (Fig. 1(a)). V_{ON} decreased significantly as t_p increased, but V_{OFF} did not change within the standard deviation of the experimental values. Figure 2(a) shows an example of the t_p-dependence of V_{ON} and V_{OFF} for room temperature and a fixed $R_{load} = 1$ kΩ. V_{ON} decreased from $\sim$50 to $\sim$25 V (red closed circles), whereas V_{OFF} remained almost constant at $\sim$20 V (blue open circles), when t_p increased from 10^{-3} s to 10^2 s, as shown in Fig. 2(a).

We then investigated the dependence of V_{ON} and V_{OFF} on the environmental temperature, T_e, using a probe station equipped with liquid nitrogen. We found that both V_{ON} and V_{OFF} decreased as T_e increased. Figure 2(b) shows an example of the T_e-dependence of V_{ON} and V_{OFF} for a fixed $t_p = 0.1$ s and $R_{load} = 1$ kΩ. V_{ON} decreased from $\sim$58 to $\sim$38 V (red closed circles), and V_{OFF} also decreased from $\sim$25 to $\sim$20 V (blue open circles), when T_e increased from 240 to 290 K.

We investigated the R_{load}-dependence of V_{ON} and V_{OFF} in the range of 500 $\Omega \leq R_{load} \leq 2000$ Ω and observed that both V_{ON} and V_{OFF} increased as R_{load} increased. In this case, R_{load} was smaller than the in-plane resistance of the insulating VO$_2$ thin film and larger than that of the metallic VO$_2$ thin film. Figure 2(c) shows an example of the R_{load}-dependence of V_{ON} and V_{OFF} for room temperature and a fixed $t_p = 0.1$ s. V_{ON} increased from $\sim$31 to $\sim$46 V (red closed circles), and V_{OFF} also increased from $\sim$15 to $\sim$29 V (blue open circle), when R_{load} increased from 500 to 2000 Ω (Fig. 2(c)).

The origin of the conductance transition of VO$_2$ thin films triggered by an electric stimulus is still debatable.[1,8–13] Some researchers suggest that the transition occurs by purely electric-field-driven phase transitions.[1,8–10] Other research groups have attributed the thermally induced phase transition to Joule heating, due to a referential experiment that revealed a sudden metal–insulator transition near 340 K in VO$_2$ films.[1,11–13] If we consider only the electric-field-driven phase transition as the origin for our experimental results, then it is hard to understand the t_p- and T_e-dependences for the switching voltages because the electric field strength does not depend on them. Note that the RC time for the electric circuit in our experiments was on the order of 10 ns. Thus, the electric-field distribution over the entire circuit immediately relaxed within the experimental time range ($\geq$1 ms). This indicated that the RC time is not the origin of the t_p-dependence. As a result, the metal–insulator transition observed in our experiments could be attributed to thermally induced phase transition by Joule heating.
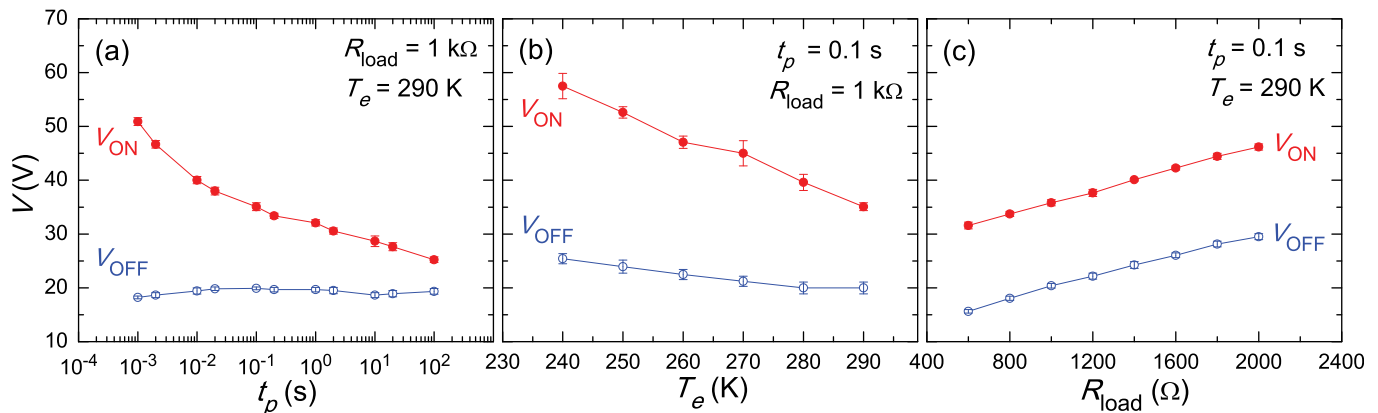

FIG. 2. Dependence of V_{ON} and V_{OFF} on (a) the period of the triangular-waveform voltage signal, t_p, (b) the environmental temperature, T_e, and (c) the resistance of the load resistor, R_{load}.

We performed numerical simulations based on the mechanism of the thermally induced metal–insulator transition to quantitatively understand the observed variation in the switching voltages. In the simulations, a two-dimensional lattice for the VO_2 thin film was assumed, whose lengths in the x- and y-directions were $L_x = 200\,\mu m$ (40 divisions) and $L_y = 25\,\mu m$ (1 division), respectively, as shown in the inset of Fig. 3(a). Note that the film thickness was set to 100 nm. We confirmed that the number of divisions in the L_y direction had no significant effect on the simulation results. The three-dimensional lattice for Al_2O_3 was attached under the VO_2 lattice, whose thickness was 1 mm (30 divisions for feasible calculation). We assumed that all of the VO_2 cells in the lattice were in the insulating state at the beginning of the simulation and were held at a temperature of T_e. With this initial configuration, the external voltage V_{ext} increased over time, starting from zero. The current density, j_n, flowing through a cell indexed by n, is given by the Ohm's law. Here, the current was assumed to flow along the direction perpendicular to the electrode, only in the VO_2 layer. To investigate the time evolution of the temperature profile, we solved the heat equation[14,15]

$$c_p^n \rho_n \partial T_n / \partial t = \nabla \cdot (\kappa_n \nabla T_n) + j_n^2 / \sigma_n, \qquad (1)$$

where c_p^n, ρ_n, κ_n, and σ_n are the specific heat, density, thermal conductivity, and electric conductivity of a cell indexed

by n, respectively. Here, T_n is the temperature at the center of the cell n. The time-step increment was fixed at 10^{-9} s for all simulations. We assumed that the heat-diffusion effect was negligible at the electrodes and that the cells in contact with the ambient surroundings were cooled by air convection. To account for the thermally induced phase transition in our simulation, the following switching rules were used for the state of the VO_2 cell:

$$\text{Insulator} \rightarrow \text{metal when } T_n > T_c,$$

$$\text{Metal} \rightarrow \text{insulator when } T_n < T_c.$$

For the VO_2 thin film, $T_c = 340$ K. The κ and σ values of the VO_2 cell depended on its state; we used $\kappa_i = 3.5$, $\kappa_m = 6$ W $(mK)^{-1}$, and $\sigma_i = 300$, $\sigma_m = 2 \times 10^5\,\Omega^{-1}\,m^{-1}$ (Refs. 11–13), where index i and m denote insulator and metal, respectively. We used $c_p = 690$ J $(kg \cdot K)^{-1}$ and $\rho = 4340$ kg m^{-3} for VO_2 and $c_p = 880$ J $(kg \cdot K)^{-1}$, $\rho = 4000$ kg m^{-3}, and $\kappa' = 45$ W $(mK)^{-1}$ for Al_2O_3.

When a triangular-waveform voltage signal with $V_{max} = 60$ V was applied, our simulation resulted in the threshold-switching $I(t)$–$V(t)$ curve, with abrupt current jumps at V_{ON} and V_{OFF}, as shown in Figs. 3(a) and 3(b). Figure 3(c) shows the sequential channel formation and T_n-distribution when the threshold-switching (Fig. 3(b)) occurred. With zero voltage bias, $T_n = T_e$ ($<T_c$) and there was no metallic channel, as shown in the first snapshot. When $V(t) > V_{ON}$, T_n of some cells reached a temperature higher than T_c due to Joule heating; a local channel formed, as shown in the second snapshot. Further increases in $V(t)$ led to an increase in the channel width (the third snapshot), while the channel width decreased as $V(t)$ decreased (the fourth snapshot). Finally, when $V(t) < V_{OFF}$, T_n for all of the cells became lower than T_c, and the channel disappeared, as shown in the fifth snapshot. The simulated metallic channel formation agreed well with experimental observation, as shown in Fig. 1(c).

Figure 4(a) shows the simulated t_p-dependence of V_{ON} and V_{OFF}. Similar to the experimental results in Fig. 2(a), V_{ON} decreased as t_p increased; however, V_{OFF} showed no apparent change. The importance of Al_2O_3 should be noted; without the Al_2O_3 lattice, the temperature of the VO_2 film would rise too fast, and the simulation would be unable to reproduce the experimental results quantitatively. To understand the simulated t_p-dependence analytically, consider a "lump" of VO_2 directly connected to the heat bath held at temperature T_e. Equation (1) can then be written as follows:

$$C dT/dt = -\frac{1}{R_{th}}(T - T_e) + V_{VO_2}^2/R, \qquad (2)$$

where C, T, R_{th}, and R are the heat capacitance, temperature, effective thermal resistance, and resistance of the VO_2 film.[16] V_{VO_2} is the applied voltage to the VO_2 thin film, which is given by $R V_{ext}/(R + R_{load})$. Note that $R = R_i$ and $R = R_m$ when VO_2 is in an insulating and metallic state, respectively. $V_{ext} = 2V_{max}t/t_p$ for $t < t_p/2$ and $V_{ext} = 2V_{max}(1 - t/t_p)$ for $t > t_p/2$. Because Eq. (2) is a first differential equation, it can be easily solved. In particular, for $t < t_p/2$, one can show that
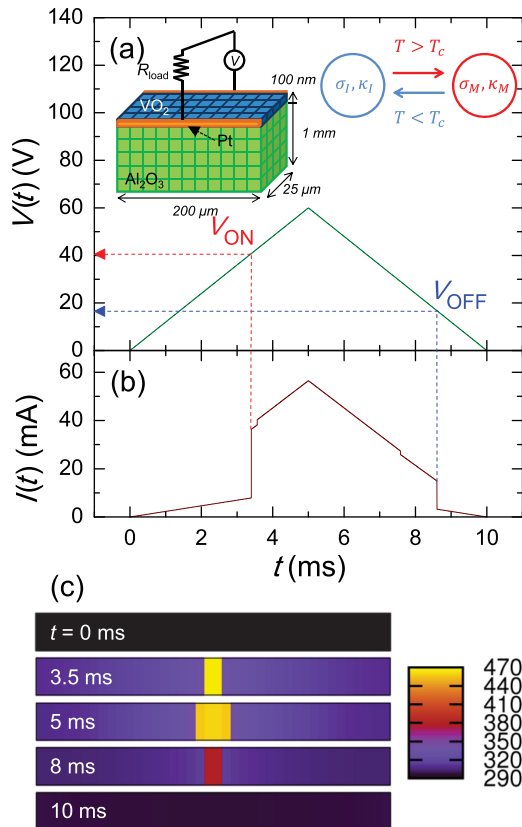

FIG. 3. Numerical simulation based on the mechanism of thermally induced phase transition. (a) Triangular-waveform voltage signal $V(t)$ and (b) resulting current $I(t)$. Insets show three-dimensional lattice of $Pt/VO_2/Al_2O_3$ sample and switching rules for the state of the VO_2 cell, which we considered for numerical simulation. (c) Procedure for the formation of a metallic channel and T_n-distribution on the surface of the thin film.
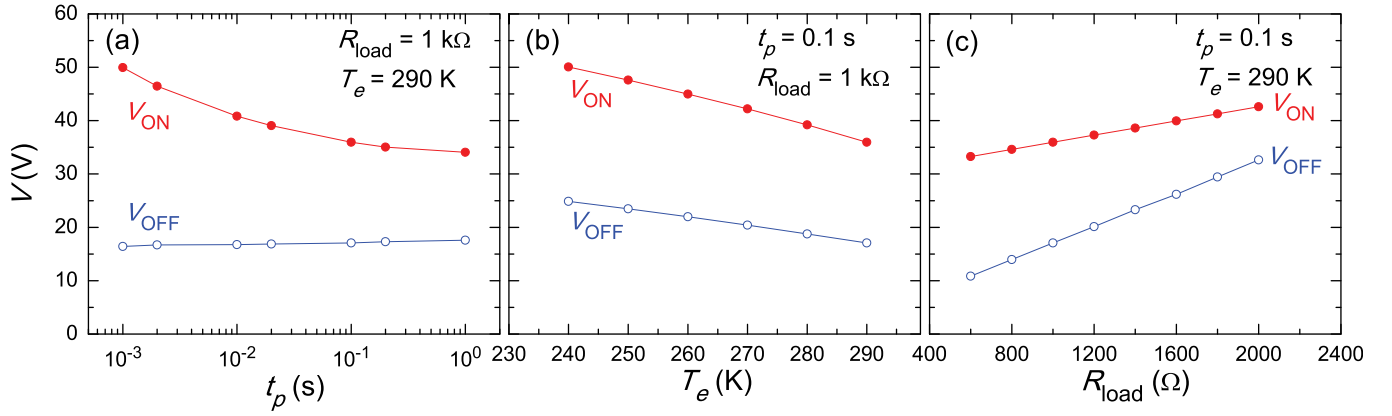
FIG. 4. Numerical simulation based on the mechanism of thermally induced phase transition. Dependence of V_{ON} and V_{OFF} on (a) t_p, (b) T_e, and (c) R_{load}.

$$V_{ON} \approx \begin{bmatrix} \mathcal{A} t_p^{-\frac{1}{3}}, & \text{for} \quad t_p \ll CR_{th}\left(\mathcal{A} = [6C(T_c - T_e)(R_i + R_{load})^2 V_{max}/R_i]^{\frac{1}{3}}\right) \\ \mathcal{B}, & \text{for} \quad t_p \gg CR_{th}\left(\mathcal{B} = [(T_c - T_e)(R_i + R_{load})^2/(R_i R_{th})]^{\frac{1}{2}}\right) \end{bmatrix}. \quad (3)$$

In the intermediate t_p region, one can numerically show that V_{ON} is a decreasing function of t_p. This decreasing-and-after-saturation behavior of V_{ON} corresponds to the simulation results, as shown in Fig. 3(a). Equating $\mathcal{B}$ in Eq. (3) and the saturation value for V_{on} (~30 V) in Fig. 3(a) gives $R_{th} \sim 300$ sK/J. Note that V_{ON} in Fig. 2(a) seems to decrease further, rather than saturate. We think that this originates from the effectively larger C due to the larger environment, which includes the connected substrate and VO$_2$ film in the actual experiment. For $t > t_p/2$, after some calculation, one can show that

$$V_{OFF} \approx \mathcal{B}', \quad \text{for} \quad t_p \gg CR_{th}\left(\mathcal{B}' = [(T_c - T_e)(R_m + R_{load})^2/(R_m R_{th})]^{\frac{1}{2}}\right). \quad (4)$$

Plugging $R_{th} \sim 300$ sK/J into Eq. (4) gives $\mathcal{B}' \sim 20$ V, which corresponds to the saturation value for V_{OFF} in the simulation. These analytic results clearly demonstrate that V_{ON} and V_{OFF} are determined by thermal processes resulting from Joule heating.

Figure 4(b) shows the T_e-dependence of V_{ON} and V_{OFF}. Both V_{ON} and V_{OFF} decreased with increasing T_e, as we observed experimentally in Fig. 2(b). These behaviors can be easily understood from Eqs. (3) and (4). Figure 4(c) shows the R_{load}-dependence of V_{ON} and V_{OFF}. Both V_{ON} and V_{OFF} increased with an increase of R_{load}, as experimentally shown in Fig. 2(c). This can also be understood from Eqs. (3) and (4). The agreement between the numerical simulations and the experimental results indicates that the variation in switching voltages of threshold-switching in VO$_2$ thin film has a thermal origin.

In summary, we explored the effect of various external parameters on the switching voltages for threshold-switching in VO$_2$ thin films. When we applied a triangular-waveform voltage signal, we observed that V_{ON} decreased with an increase of t_p. For a fixed t_p, we observed that both V_{ON} and V_{OFF} decreased (or increased) as T_e (or R_{load}) increased. A simulation based on the mechanism of thermally induced phase transition reproduced all of the experimental results quantitatively. We also gave a simple analytic explanation for the simulation results. Thus, our simulation and analytic results demonstrate that variation in switching voltages originates from thermal processes induced by Joule heating and

its dissipation, i.e., the switching voltages for VO$_2$ threshold-switching can be intentionally controlled or accidentally changed by variation of the thermal environment. This indicates the importance of thermal architecture for stable performance of VO$_2$ applications.

[1]N. F. Mott, Rev. Mod. Phys. **40**, 677 (1968).
[2]M. Imada, A. Fujimori, and Y. Tokura, Rev. Mod. Phys. **70**, 1039 (1998).
[3]M.-J. Lee, Y. Park, D.-S. Suh, E.-H. Lee, S. Seo, D.-C. Kim, R. Jung, B.-S. Kang, S.-E. Ahn, C. B. Lee, D. H. Seo, Y.-K. Cha, I.-K. Yoo, J.-S. Kim, and B. H. Park, Adv. Mater. **19**, 3919 (2007).
[4]S. H. Chang, S. B. Lee, D. Y. Jeon, S. J. Park, G. T. Kim, S. M. Yang, S. C. Chae, H. K. Yoo, B. S. Kang, M.-J. Lee, and T. W. Noh, Adv. Mater. **23**, 4063 (2011).
[5]K. Kato, P. K. Song, H. Odaka, and Y. Shigesato, Jpn. J. Appl. Phys. **42**, 6523 (2003).
[6]M. Seo, J. Kyoung, H. Park, S. Koo, H.-S. Kim, H. Bernien, B. J. Kim, J. H. Choe, Y. H. Ahn, H.-T. Kim, N. Park, Q.-H. Park, K. Ahn, and D.-S. Kim, Nano Lett. **10**, 2064 (2010).
[7]T. Driscoll, H.-T. Kim, B.-G. Chae, B.-J. Kim, Y.-W. Lee, N. M. Jokerst, S. Palit, D. R. Smith, M. Di Ventra, and D. N. Basov, Science **325**, 1518 (2009).
[8]G. Gopalakrishnan, D. Ruzmetov, and S. Ramanathan, J. Mater. Sci. **44**, 5345 (2009).
[9]B. Wu, A. Zimmers, H. Aubin, R. Ghosh, Y. Liu, and R. Lopez, Phys. Rev. B **84**, 241410 (2011).

[10]Z. Tao, T.-R. T. Han, S. D. Mahanti, P. M. Duxbury, F. Yuan, C.-Y. Ruan, K. Wang, and J. Wu, Phys. Rev. Lett. **109**, 166406 (2012).

[11]Y. J. Chang, J. S. Yang, Y. S. Kim, D. H. Kim, T. W. Noh, D.-W. Kim, E. Oh, B. Kahng, and J.-S. Chung, Phys. Rev. B **76**, 075118 (2007).

[12]D.-W. Oh, C. Ko, S. Ramanathan, and D. G. Cahill, Appl. Phys. Lett. **96**, 151906 (2010).

[13]Y. Zhang and S. Ramanathan, Solid-State Electron. **62**, 161 (2011).

[14]S. H. Chang, S. C. Chae, S. B. Lee, C. Liu, T. W. Noh, J. S. Lee, B. Kahng, J. H. Jang, M. Y. Kim, D.-W. Kim, and C. U. Jung, Appl. Phys. Lett. **92**, 183507 (2008).

[15]S. Menzel, M. Waters, A. Marchewka, U. Böttger, R. Dittmann, and R. Waser, Adv. Funct. Mater. **21**, 4487 (2011).

[16]K. M. Kim, D. S. Jeong, and C. S. Hwang, Nanotechnology **22**, 254002 (2011).